Journal of Intelligent Systems and Internet of Things
Vol. 12, No. 01, PP. 144-157, 2024
DOI: https://doi.org/10.54216/JISIoT.120111

A Frequency Reconfigurable Graphene-Based Microstrip Antenna with Mushroom-Like EBG

Nora Ahmed Mohammed [1,*], Ghufran abdulqader alhaddad [2], Marwa S. J.[3], Hasanain Jawad Radeef [4]
[1,2,3] College of Engineering, Al-Qadisiyah University, Iraq
[4] Federal Board of supreme audit, AL- Diwaniyah, Iraq
Emails: nora.mohammed@qu.edu.iq; Ghufran@qu.edu.iq; marwa.satar@qu.edu.iq; hassanainradif78.hr@gmail.com

.

Abstract

The growing demand for wireless applications has led to network congestion issues. In response, network operators have recommended a transition to higher frequencies, particularly within the unlicensed millimeter-wave (mm-wave) spectrum. This shift aims to fulfill users' desires for rapid data transmission within personal networks, whether at home or in the office, exemplified by technologies like WiGig technology and indoor applications. However, a significant challenge in achieving high data transfer speeds within this frequency range lies in the design of the antenna. These antennas must strike a balance between size and performance. Microstrip Patch (MP) antennas have gained recognition for their compact form and seamless integration into mobile communication systems. Nonetheless, they grapple with limitations such as poor gain and narrow bandwidth, largely attributable to surface waves negatively impacting antenna performance. In this study, we introduce, design, and optimize an MP antenna tailored for 60 GHz applications. To enhance the performance of the MP antenna, we introduce various mushroom-like Electromagnetic Bandgap (EBG) structures. These structures address the propagation of the surface waves issue that affects the antenna performance. Additionally, to create a tunable frequency antenna the variable conductivity of the graphene material is used in the form of implanted slots on the patch and tuned by applied DC voltage on the slots. Finally, the parameters of the MP antenna undergo enhancement based on simulation results obtained through CST software.

Received: August 15, 2023 Revised: November 22, 2023 Accepted: March 08, 2024

Keywords: MP antenna; Millimeter-wave; WiGig; License-free spectrum

1. Introduction

Wireless communication, once a theoretical concept, has become a tangible reality in both general-purpose applications and industrial automation. It is no longer confined to academic discussions. In fact, a growing number of industries and manufacturing companies have already embraced wireless instrumentation within their facilities. Wireless instruments are becoming an indispensable component of industrial automation, akin to how cell phones are essential in the field of telecommunications [1].

The advantages of wireless instrumentation and the associated data acquisition and control systems are driving industries to adopt this technology. Wireless communication can be defined as the exchange of information or data among two or more devices without the need for physical conductor wires to facilitate the communication process. This evolution reflects the natural progression towards efficient and wire-free connectivity [2].

Several bands of frequency are employed for various wireless communication applications, it's important to note that the surge in wireless connectivity across established networks has brought about challenges such as network congestion. To address this issue, wireless network operators have proposed a solution involving the utilization of high-frequency bands. This strategic shift not only aligns with users' desires for enhanced data transmission speeds but also aims to alleviate congestion woes within wireless networks [3].

One particularly promising avenue in this pursuit of high-speed wireless communication lies in millimeter waves. These waves offer a substantial bandwidth, resulting in rapid data transfer rates. Additionally, a largely untapped resource exists within the frequency spectrum, specifically within the range of 57-66 GHz, as illustrated in Figure 1. Commonly referred to as the license-free band, this spectrum presents a valuable opportunity for enhancing wireless connectivity further [4].

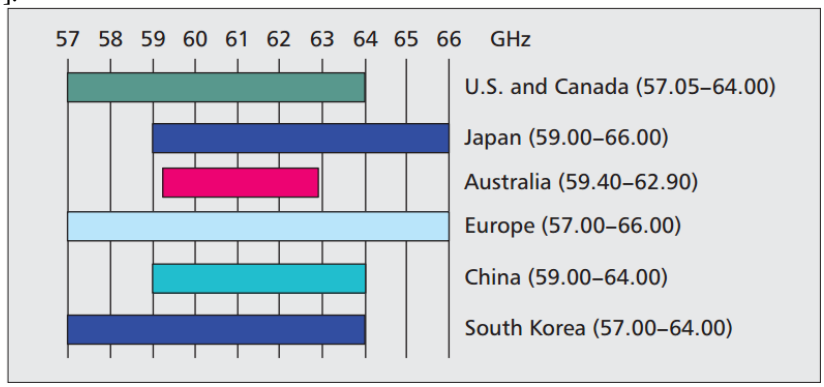

Figure 1: Frequency spectrum of the license-free.

The use of the license-free frequency spectrum has made Microstrip Patch (MP) antennas indispensable tools. The 57-66 GHz frequency band, which is distinguished by its lack of licencing restrictions, is made possible in large part by these small, effective antennas. They are ideal for a variety of applications because of their compact form size and simplicity of integration, including as wireless instrumentation, industrial automation, and personal networks in homes and businesses [5].

The propagation of mm-waves within the 57-66 GHz range, particularly in the license-free spectrum, presents both opportunities and challenges in wireless communication. One significant challenge stem from the inherent susceptibility of mm-waves to atmospheric absorption and attenuation, as presented in Figure 2.

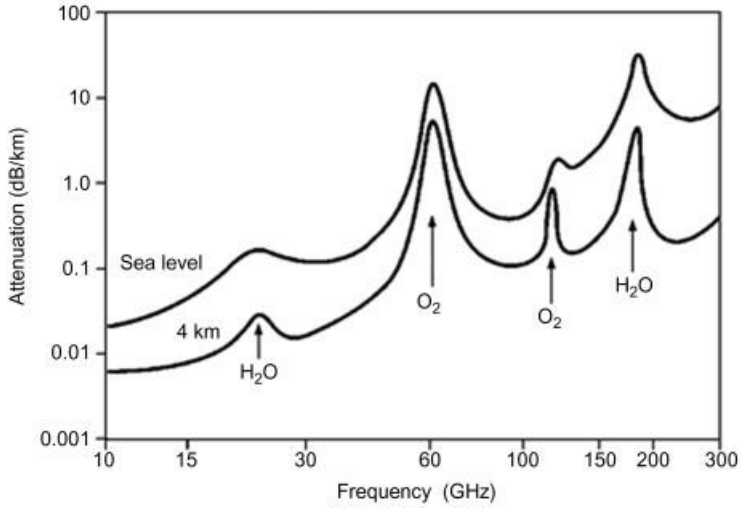

Figure 2: Average atmospheric absorption in mm-waves.

These waves are highly absorbed by atmospheric gases, notably oxygen, and water vapour, leading to considerable signal attenuation over distances. This characteristic necessitates careful planning and deployment strategies to ensure reliable coverage, especially in urban environments where signal blockage by buildings and foliage is common. Moreover, the shorter wavelengths of mm-waves result in limited penetration through obstacles such as walls and structures, posing obstacles to indoor coverage and requiring the deployment of additional infrastructure to ensure seamless connectivity. Additionally, mm-waves are more susceptible to signal degradation due to phenomena like rain fade, further complicating their propagation in outdoor environments. Despite these challenges, the license-free nature of the spectrum offers opportunities for innovation and experimentation in various applications, including high-speed wireless broadband, point-to-point communication links, and wireless backhaul solutions. Overcoming the propagation challenges of mm-waves in the 57-66 GHz range demands advancements in antenna technology, signal

processing techniques, and network optimization strategies to fully harness their potential for next-generation wireless communication systems [6].

Using MP antennas to their full ability within this spectrum presents a number of issues, one of which is maximising their performance to enable dependable data transfer. Surface waves are one obstacle that engineers and scientists are always working to overcome in order to increase the gain and bandwidth of these antennas. To expand the possibilities of microstrip antennas inside the license-free frequency band, methods like the inclusion of Electromagnetic Bandgap (EBG) structures [7] and the use of cutting-edge materials like graphene for frequency tweaking have been investigated. As a result, microstrip antennas are in a prime position to play a crucial role in realising the license-free spectrum's full potential and allowing high-speed wireless connectivity in a variety of applications [9].

The field of reconfigurable microstrip antennas has substantially advanced with the incorporation of graphene material [10]. With its exceptional electrical, thermal, and mechanical qualities, graphene has emerged as a major advancement in antenna technology. It enables the dynamic tuning and reconfiguration of antenna parameters, including resonant frequency, bandwidth, and radiation patterns, when used with microstrip antennas [11]. This versatility is made possible by graphene's special ability to control its conductivity by applying a voltage. Researchers can carefully modify the antenna's performance to satisfy particular communication requirements by carving tiny slots on the antenna patch and altering the voltage [12].

Reconfigurable microstrip antennas based on graphene offer improved efficiency and versatility in addition to more adaptability to changing communication needs [13]. They are used in a variety of fields, including radar and remote sensing technologies as well as wireless communication systems. By enabling real-time modifications that maximise antenna performance, this use of graphene material represents a substantial advancement in antenna design [14], [15]. As a result, antennas are now priceless tools for cutting-edge wireless communication systems and beyond.

MP antennas' use of EBG structures that resemble mushrooms and graphene material has significant promise for improving antenna performance and promoting invention in the area of electromagnetic engineering. EBG structures are well known for their capacity to suppress surface waves and improve antenna radiation characteristics. These structures were inspired by the special electromagnetic properties of mushrooms. By incorporating graphene, renowned for its exceptional conductivity and mechanical properties, into these EBG structures, microstrip antennas can achieve improved impedance matching and reduced losses, resulting in enhanced radiation efficiency. This synergy between mushroom-inspired EBG structures and graphene material not only opens new horizons for the design of high-performance microstrip antennas but also contributes to the development of eco-friendly and sustainable communication systems, aligning with the global push for green technology solutions [16-20, 28-34].

In this work, a small size MP antenna is proposed to be designed and simulated for the applications of indoor communications based on 60 GHz. In order to enhance the performance of the proposed MP antenna and eliminate the effect of the surface waves that deteriorate the MP antenna performance the structure of the mushroom-like EBG is used. Additionally, to create a frequency-tuning property in the proposed MP antenna small layers of graphene are implanted at the rectangular patch which is tuned by DC voltage, whereas, by changing the applied voltage the MP antenna is operated with a different frequency band.

2. MP Antenna Structure

Radar and wireless communication systems both make extensive use of the underlying microstrip antenna construction. It consists of a ground plane on one side and a radiating patch—typically a tiny metallic element-placed atop a dielectric substrate, as shown in Figure 3. Compact size, low profile, ease of fabrication, and adaptation for different frequency bands are just a few benefits of this straightforward yet adaptable arrangement. To produce desired frequency characteristics and radiation patterns, the ground plane's form, the radiating patch's size, and the substrate's dimensions can all be customized. Microstrip antennas can also be created for single or dual polarization, making them appropriate for a variety of uses, including RFID systems and satellite communication. The microstrip antenna's status as a crucial part of contemporary wireless technology has been cemented by their adaptability and effectiveness in sending and receiving electromagnetic signals [21].

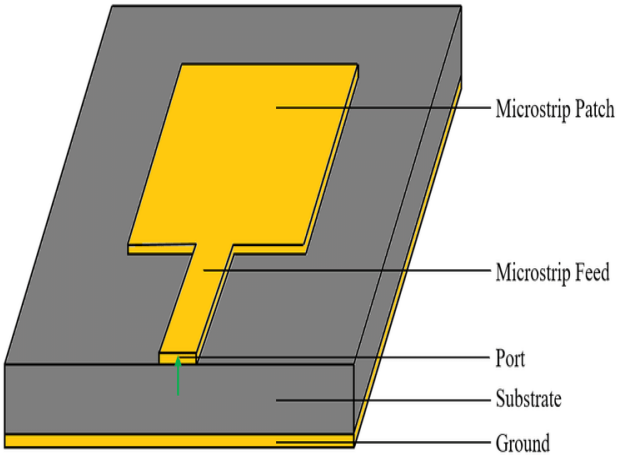

Figure 3: Structure for MP antenna.

3. Proposed MP Antenna Design

In order to start the proposed MP antenna design, the primary step is the design of a regular MP antenna by selecting the primary parameters that are set in Table 1.

Table 1: Fundamental parameters for antenna design.

Parameter	Value
MP antenna operating frequency (f_o)	60 GHz
Dielectric constant for the substrate (ε_r)	2.2 (unitless)
Height of the substrate (h)	0.1mm

After setting the primary parameters, the dimensions for the MP antenna must be determined by the MATLAB code designed to solve the following equations [22]:

$$W_p = \frac{C_o}{2f_o\sqrt{\frac{(\epsilon_r+1)}{2}}} \quad (1)$$

$$\epsilon_{re} = \frac{\epsilon_r+1}{2} + \frac{\epsilon_r-1}{2}\left[1+12\frac{h_s}{W_p}\right]^{\frac{-1}{2}} \quad (2)$$

$$\Delta L = 0.412h\frac{(\epsilon_{re}+0.3)\left[\frac{W_p}{h_s}+0.264\right]}{(\epsilon_{re}-0.258)\left[\frac{W_p}{h_s}+0.8\right]} \quad (3)$$

$$L_e = \frac{C_o}{2f_o\sqrt{\epsilon_{re}}} \quad (4)$$

$$L_p = L_e - 2\Delta L \quad (5)$$

$$W_s = 2\times W_p \quad (6)$$

$$L_s = 2\times L_p, \quad (7)$$

Where W_p is the patch width, C_o is the speed of light, f_o is the resonant frequency, ϵ_r is the relative permittivity, h_s is the substrate height, L_e is the effective length, ΔL is the length expansion, W_s is the substrate width, and L_s is the substrate length.

Once the traditional rectangular MP antenna's dimensions have been calculated, the simulation phase commences using specialized CST software designed for antenna simulations. Figure 4 showcases the conventional rectangular MP antenna within the CST simulation environment.

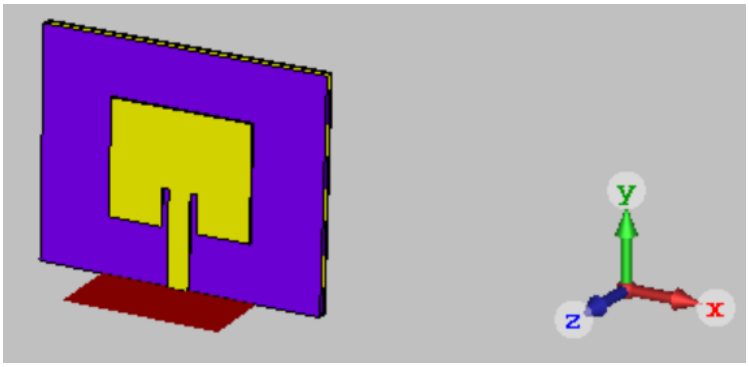

Figure 4: Simulated MP antenna within CST.

Following the simulation of the traditional rectangular MP antenna within the CST package, it becomes evident that there is an impedance mismatch issue. To address this concern, we employ a parameter sweeping process, involving iterative adjustments to the dimensions of the traditional MP antenna to optimize its performance. Table 2 presents the selected parameter values for the traditional MP antenna following the parameter sweep.

Table 2: Dimensions for the traditional MP antenna after the parameter sweep.

Parameters	Parameters by Equations (mm)	Parameter Sweep (mm)
Width of the Patch (W_p)	2.009	2.0
Length of the Patch (L_p)	1.668	1.631
Width of the Substrate (W_s)	4.0162	4.05
Length of the Substrate (L_s)	3.3363	3.26
Separation spacing between patch and feed (Ga)	0.0181	0.12
Feed inserting in the patch (F_i)	0.58219	0.53
Feeding Line Length (L_{feed})	1.80015	1.81
Feeding Line Width (W_{feed})	0.30807	0.311

4. MP Antenna with EBG Cells

When the MP antennas are energized with an electrical signal, surface waves propagate across the dielectric substrate of the antenna. These waves can significantly degrade various antenna parameters, including antenna gain, efficiency, and bandwidth, ultimately affecting antenna performance [23]. To mitigate this issue, several approaches can be employed, with one of the most prominent methods being the utilization of a mushroom-like EBG configuration [24]. In this approach, a conductive structure is printed onto the same substrate and strategically positioned around the antenna patch. The EBG cells are directly connected to the ground plane through connecting vias. This configuration serves as a passive filter, effectively minimizing or eliminating the adverse effects of surface waves [25], as depicted in Figure 5.

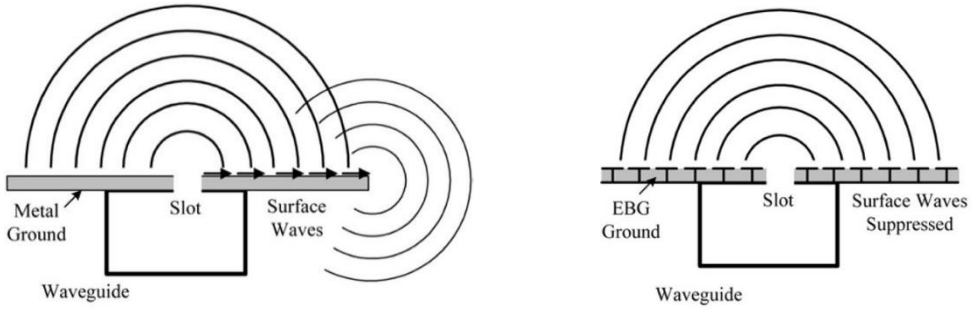

(a) Without EBG cells (b) With EBG cells

Figure 5: Surface waves distribution over the MP antennas.

Typically, EBG cells are often symbolized as lumped elements consisting of an inductor (L) and a capacitor (C), as illustrated in Figure 6. Consequently, EBG cells can be conceptualized as LC resonators. Mathematically, the modeling of EBG cells can be achieved using the set of the following equations [26]:

$$C = \frac{W \in_r (1 + \in_r)}{\pi} \operatorname{sech}^{-1}\left(\frac{W+g}{W}\right) \quad (8)$$

$$L = 2 \times 10^{-7} h \left[\ln\left(\frac{2h}{r}\right) + 0.5\left(\frac{2r}{h}\right) - 0.75\right] \quad (9)$$

$$f_o = \frac{1}{6.28\sqrt{LC}} \quad (10)$$

In these equations, the variables are defined as follows, C is represents the capacitance associated with the EBG cells, L is represents the inductance corresponding to the EBG cells, W signifies the width of the EBG cell, g denotes the spacing between adjacent cells, h indicates the total height of the MP antenna, and r represents the radius of the connecting via.

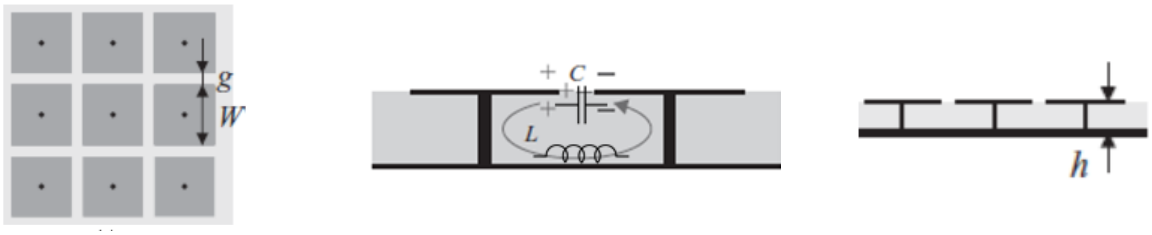

(a) Front view (b) Equivalent EBG cells circuit (c) Side view

Figure 6: Arrangement of the mushroom-like EBG configuration.

After optimizing the traditional MP antenna, a mushroom-like EBG configuration is employed to suppress the surface waves excited by the radiated patch of the antenna while also contributing to gain improvement. In the previous design of the traditional rectangular MP antenna, a square mushroom-like EBG 3×1 array configuration is integrated on each of its sides, as illustrated in Figure 7.

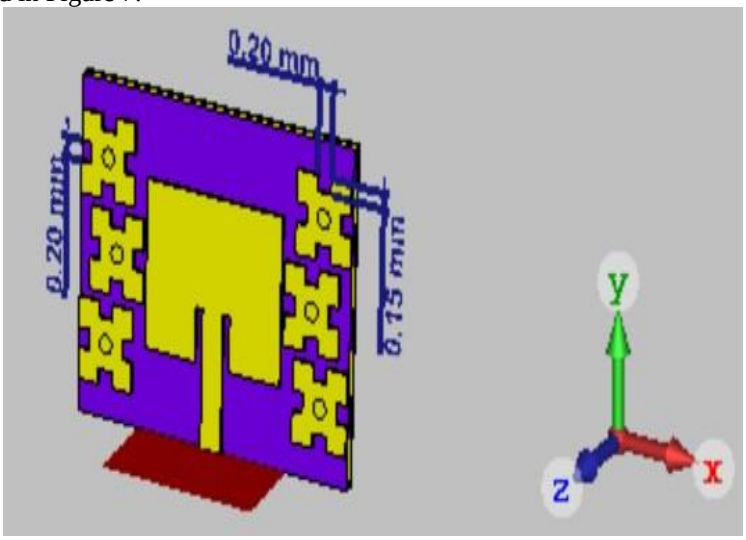

Figure 7: Simulated MP antenna with EBG cells.

To provide greater clarity, by using Microsoft Office a graphical representation has been created as shown in Figure 8, which was introduced for the purpose of illustrating the parameters of mushroom-shaped cells. The dimensions of the mushroom-like EBG cell, along with the spacings between adjacent elements, have been meticulously fine-tuned through numerous experiments to attain optimal results. Table 3 conveniently outlines these dimensions, gap measurements, and the radiated patch dimensions of the antenna.

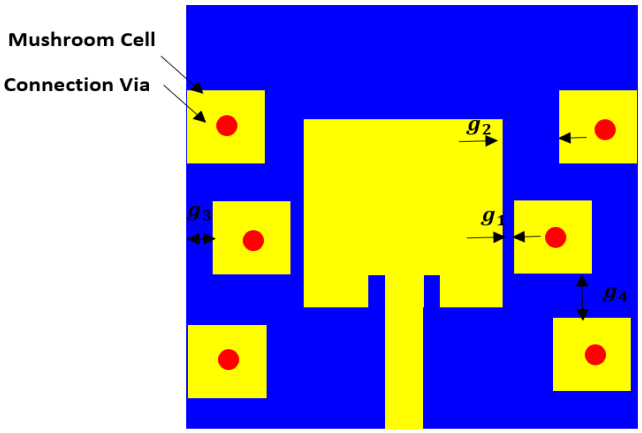

Figure 8: Graphical illustration for the MP antenna with mushroom cells.

Table 3: Dimensions and position for the mushroom like-EBG cell.

Parameter	Size (mm)
Width of single mushroom cell	0.80
Length of single mushroom cell	0.80
Diameter of cell via	0.20
Separation distance (g_1)	0.050
Separation distance (g_2)	0.20
Separation distance (g_3)	0.15
Separation distance (g_4)	0.10

To maximize the advantages derived from the incorporation of the mushroom cells, their quantity has been augmented on both sides of the radiating patch of the antenna. This augmentation, as depicted in Figure 9, results in an expansion of the antenna's overall dimensions. The conclusive dimensions of the proposed antenna, following the inclusion of these additional cells, are comprehensively presented in Table 4.

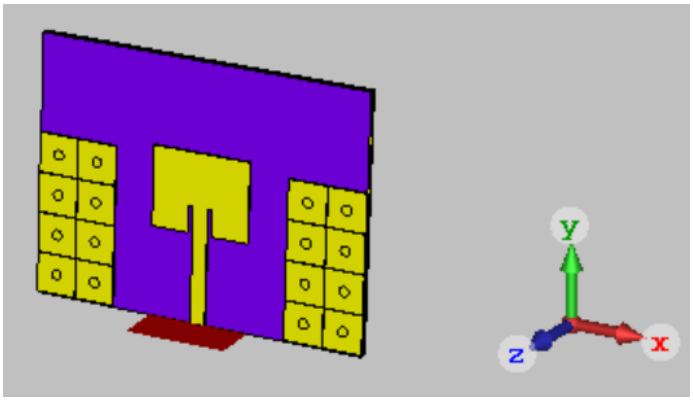

Figure 9: Simulated MP antenna loaded with the EBG cells.

Table 4: Optimized dimensions for the simulated MP antenna.

Parameters	Parameter Sweep in (mm)
Width of the Patch (W_p)	2.0
Length of the Patch (L_p)	1.630
Width of the Substrate (W_s)	7.0
Length of the Substrate (L_s)	5.26
Separation spacing between patch and feed (Ga)	0.1
Feed inserting in the patch (F_i)	0.53
Feeding Line Length (L_{feed})	1.80
Feeding Line Width (W_{feed})	0.310

5. Proposed MP Antenna with Graphene Material

To demonstrate the application of graphene material in reconfigurable antennas, our primary focus in this study centres around the rectangular MP antenna. This antenna comprises a copper patch with an embedded graphene sheet. The initial step in our design process involves strategically positioning the graphene sheets within the patch. We determine these positions by carefully analysing the distribution of surface current on the patch and identifying locations where moderate current density accumulates most effectively.

One of the exceptional characteristics of graphene material that we harness in this work is its variable surface impedance, which is directly linked to the applied DC voltage (Vdc). The graphene sheets, or implanted flakes, function as voltage-controllable switches, enabling us to manipulate the current distribution across the patch. When Vdc is increased, the impedance of the graphene flakes decreases, allowing current to flow through them. Conversely, when Vdc is decreased, the impedance of the flakes increases, permitting only leakage currents to pass. These switching states result in the antenna patch assuming a normal size in the ON state (i.e., with a high Vdc) and a smaller size in the OFF state (i.e., with a low Vdc).

This configuration results in an antenna capable of operating at multiple frequencies depending on whether it is in the ON or OFF state. For a visual representation of the current distribution across the antenna patch, please refer to Figure 10.

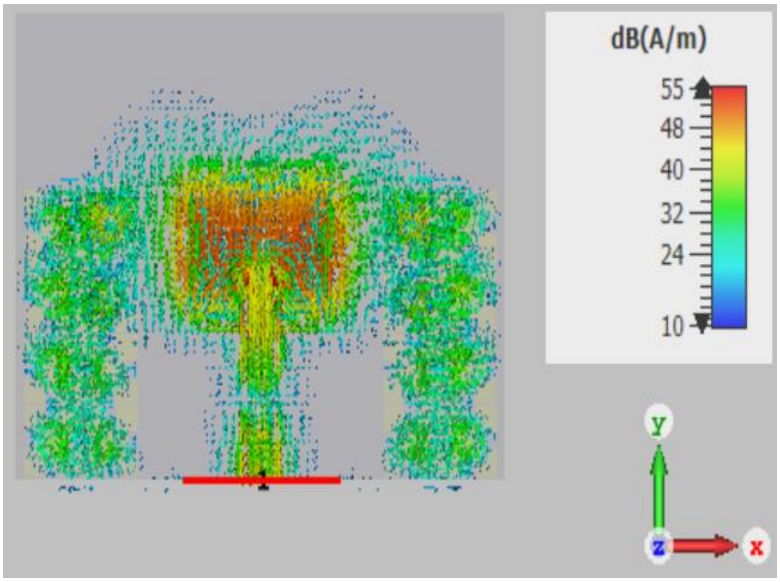

Figure 10: Distribution of current on the proposed MP antenna with EBG cells.

Following the assessment of the current distribution on the patch, we strategically implanted two graphene flakes measuring (0.4×0.4 mm^2) each. These flakes were placed on the left and right middle edges of the patch, precisely where the current distribution was optimal. This placement was chosen to minimize signal reflection. As depicted in Figure 11, the value of Vdc can be promptly applied to the graphene sheets through the antenna's feeding port.

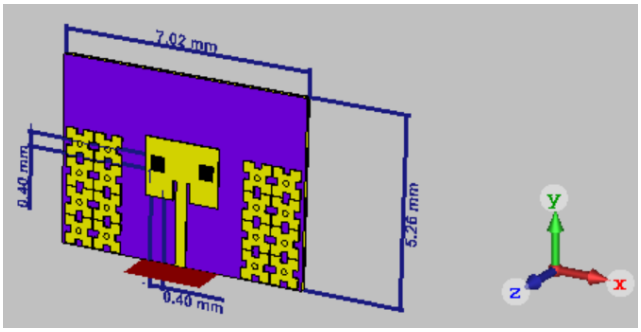

Figure 11: Simulated MP antenna with graphene sheets and EBG cells.

To model the graphene material in the CST software, we calculated the impedance of the flakes using MATLAB software, employing the following equation [27]:

$$\sigma_{AC} = \frac{-jq^2 k_B T}{\pi\hbar^2(\omega - j\tau_t^{-1})}\left(\frac{\mu_c}{k_B T} + 2ln\left(e^{-\frac{\mu_c}{k_B T}} + 1\right)\right) \quad (10)$$

Where σ_{AC} is the conductivity of the graphene material for the lower frequencies, k_B is represents the Boltzmann constant, T is referring to the room temperature, μ_c is the chemical potential for the graphene, ω is referring to the angular frequency, and $\hbar$ is the reduced Plank's constant. All the values of the constants have selected according to [28].

6. Results and Interpretation

This section of the paper is clearly interpreting the obtained results after designing and optimising the proposed MP antenna based on EBG cells and the sheets of the graphene. The obtained return loss (S_{11}) for the primary MP antenna design before the sweep for the parameter process is mismatching at the centre frequency, as shown in Figure 12.

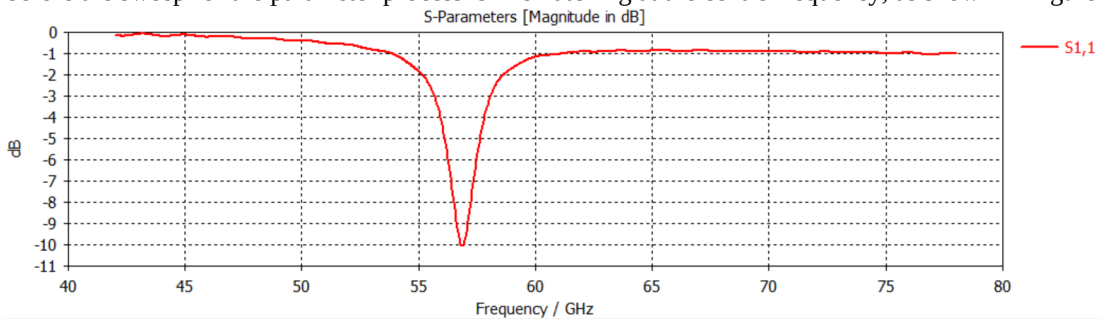

Figure 12: The S_{11} for the MP antenna before parameter sweep.

The parameter sweeps and the mushroom-like EBG cells in the shape of a matrix are used to overcome the mismatch problem, and then the S_{11} is boosted, as shown in Figure 13.

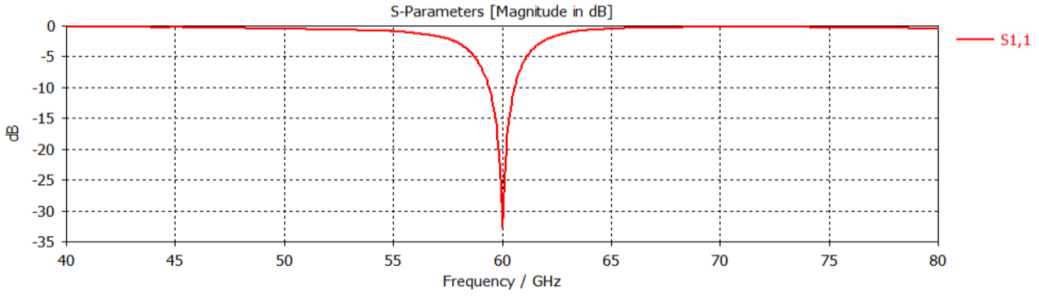

Figure 13: The S_{11} for the MP antenna after parameter sweep and adding EBG cells.

The MP antenna bandwidth is popularly measured from the S_{11} pattern at -10 dB. The bandwidth for the MP antenna with EBG cells is equal 1170 MHz, as shown in Figure 14.

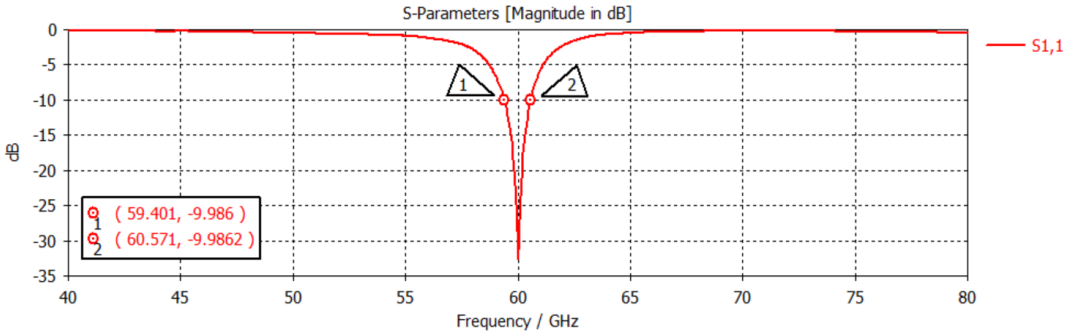

Figure 14: The bandwidth for the MP antenna after parameter sweeps and adding EBG cells.

Generally, the gain for the MP antenna is slightly low because it is affected by the characteristics of the substrate, after adding the EBG cells the gain is improved to 8.25 dBi, as shown in Figure 15.

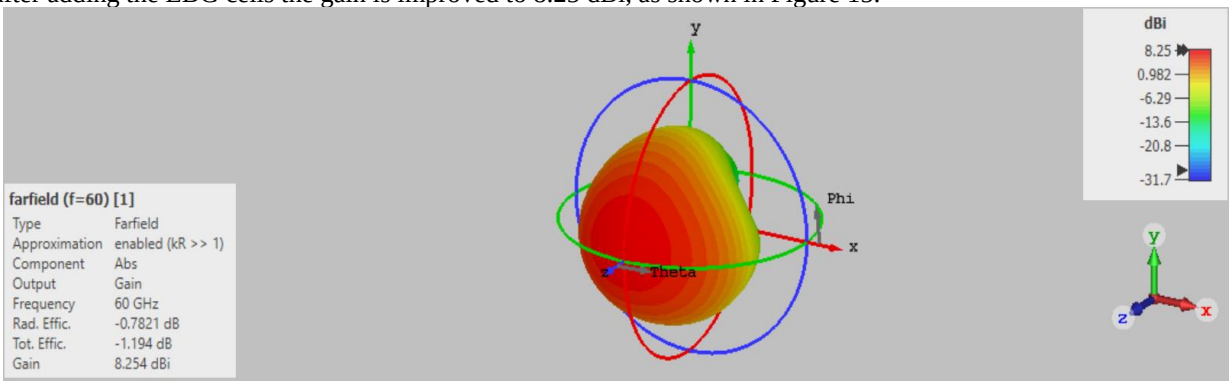

Figure 15: The bandwidth for the MP antenna after parameter sweeps and adding EBG cells.

After combining the graphene sheets with the patch of the simulated MP antenna, a dual band of frequencies of 60 GHz with an S_{11} of -29 dB and bandwidth of 1399 MHz is obtained during graphene biasing, as shown in Figures 16 and 17.

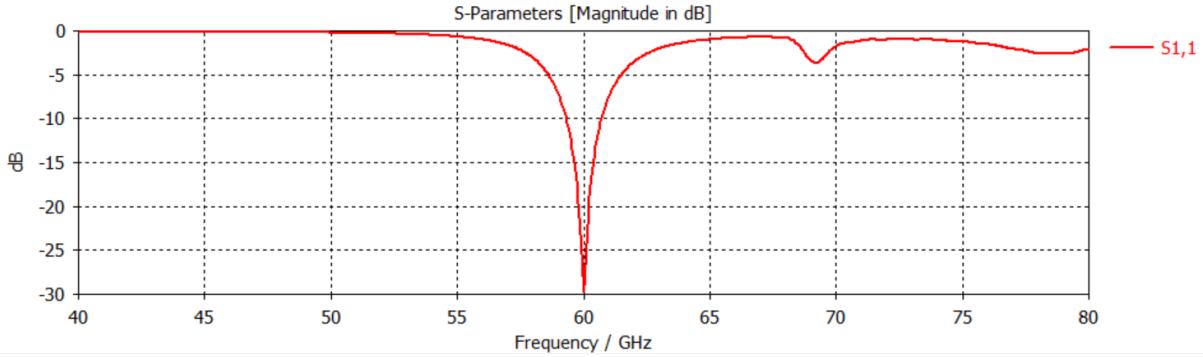

Figure 16: The S_{11} for the MP antenna at biasing case.

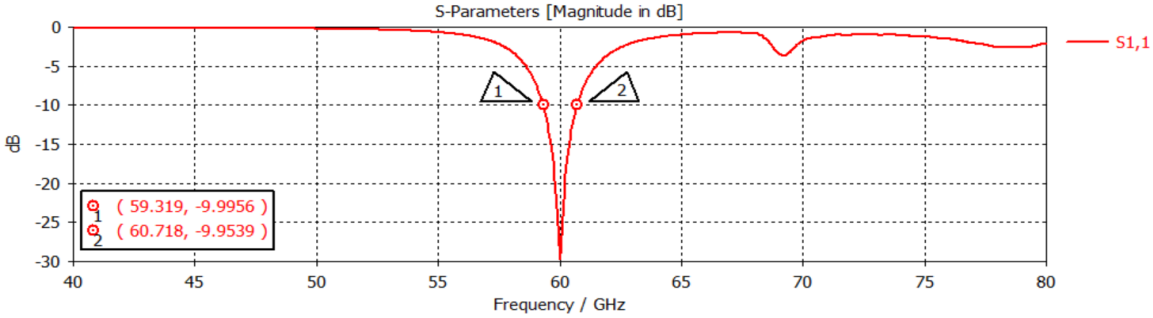

Figure 17: The bandwidth for the MP antenna at biasing case.

The second band operates at 54.5 GHz, with an S_{11} of -14.557 dB, and a bandwidth of 882 MHz in the no bias case, as shown in Figures 18 and 19.

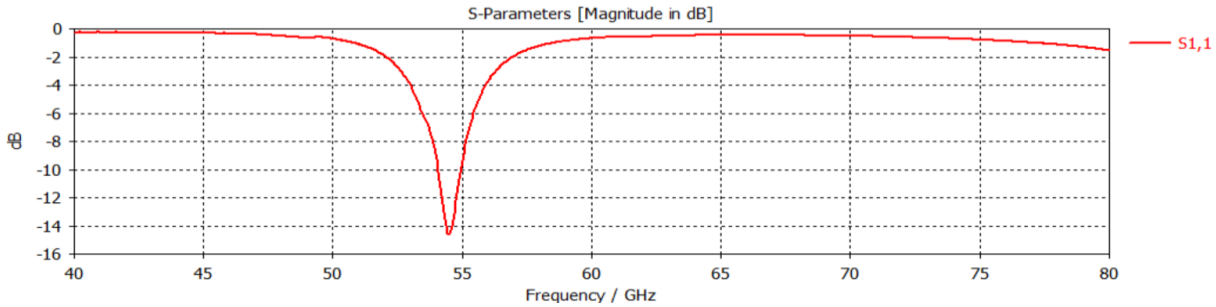

Figure 18: The S_{11} for the MP antenna at bias case.

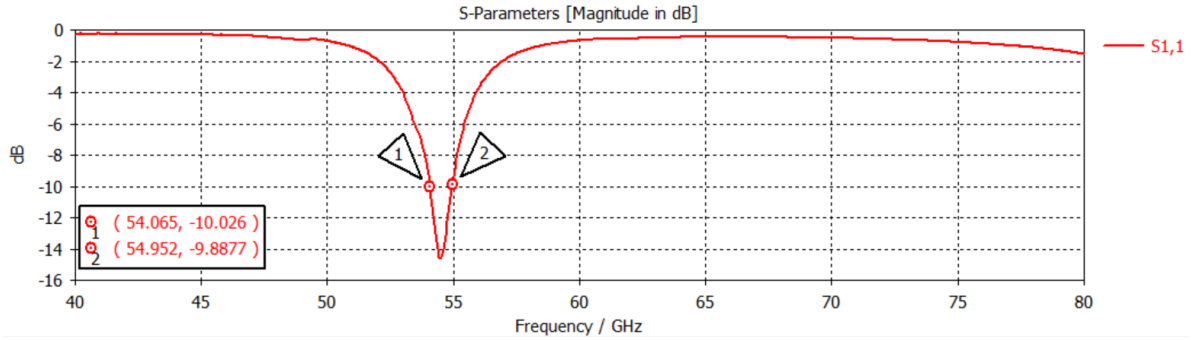

Figure 19: The bandwidth for the MP antenna at no bias case.

Finally, the gain of the simulated MP antenna with EBG cells and graphene material is variable in the biasing and no biasing situations. The gain for the MP antenna at the biasing situation is up to 6.26 dBi and 5.53 dBi at the no biasing situation, as shown in Figures 20 and 21.

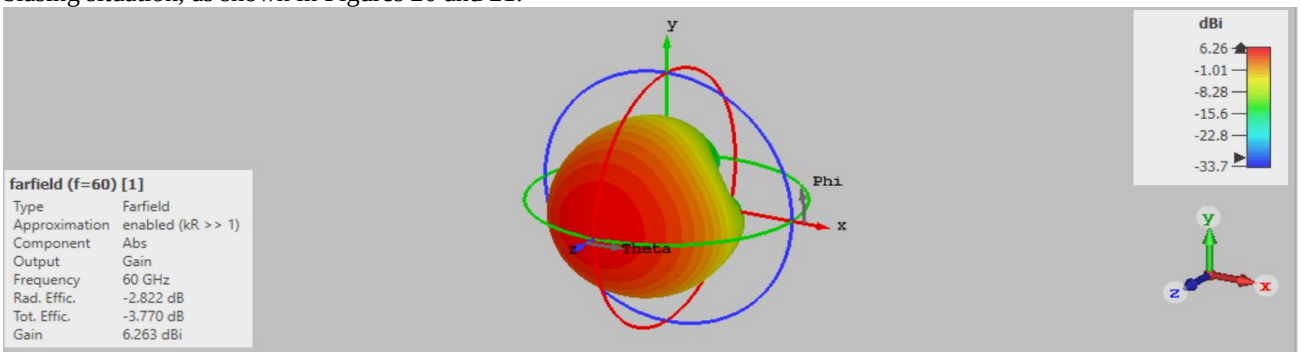

Figure 20: The gain for the MP antenna at bias case.

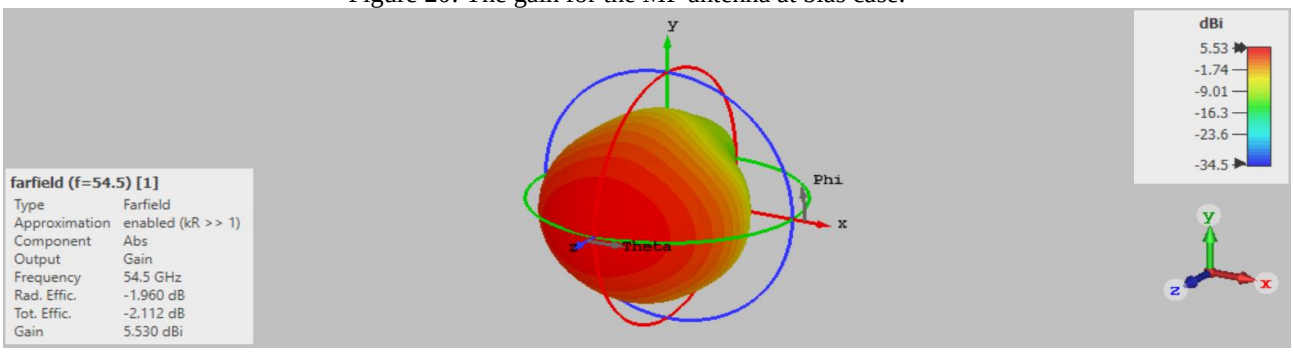

Figure 21: The gain for the MP antenna at no bias case.

7. Conclusion

As the use of wireless communication grows, as does the development of diverse applications, there is an increasing demand to shift to unlicensed high-frequency bands. The requirement to reach internet speeds that meet consumer

expectations is driving this move. Within this higher frequency range, it becomes critical to prioritise the development of small antenna designs that provide remarkable performance. The purpose of this research paper is to design, implement, and improve a tiny MP antenna for internal network applications and 5G connection. When powered, MP antennas have a significant hurdle in the form of surface wave generation, generating in losses that limit their total performance. To counteract the negative impacts of these surface waves, a mushroom-like EBG structure in the form matrix has been proposed, with the goal of achieving ideal results. Furthermore, to achieve frequency reconfigurability in the MP antenna, a variable conductivity feature has been incorporated using graphene material controlled by DC voltage. This involved embedding square graphene strips onto the antenna patch and regulating them to provide two distinct frequency bands: 54.5 GHz when no external DC bias is applied to the graphene, and 60 GHz when biased by an external DC source. Simulation results demonstrate excellent impedance matching and gain within the specified operational frequency bands.

References

[1] M. Wollschlaeger, T. Sauter and J. Jasperneite, "The Future of Industrial Communication: Automation Networks in the Era of the Internet of Things and Industry 4.0," in IEEE Industrial Electronics Magazine, vol. 11, no. 1, pp. 17-27, March 2017, doi: 10.1109/MIE.2017.2649104.

[2] F. Li, Y. Laili, X. Chen, Y. Lou, C. Wang, H. Yang, et al., "Towards big data driven construction industry," Journal of Industrial Information Integration, vol. 100483, 2023. DOI: 10.1016/j.jii.2023.100483.

[3] M. Pons, E. Valenzuela, B. Rodríguez, J. A. Nolazco-Flores, and C. Del-Valle-Soto, "Utilization of 5G Technologies in IoT Applications: Current Limitations by Interference and Network Optimization Difficulties—A Review," Sensors, vol. 23, no. 8, pp. 3876, 2023. DOI: 10.3390/s23083876.

[4] J. Xu, Z. Peng, Z. Long, et al., "Design of microstrip patch antenna element and array on quartz glass wafer with suspended cavity based on MEMS technology,"Microsyst Technol, vol. 29, pp. 835–846, 2023. DOI: 10.1007/s00542-023-05467-0.

[5] L. Zhang et al., "A Survey on 5G Millimeter Wave Communications for UAV-Assisted Wireless Networks," IEEE Access, vol. 7, pp. 117460-117504, 2019. DOI: 10.1109/ACCESS.2019.2929241.

[6] S. Rangan, T. S. Rappaport and E. Erkip, "Millimeter-Wave Cellular Wireless Networks: Potentials and Challenges," in Proceedings of the IEEE, vol. 102, no. 3, pp. 366-385, March 2022, DOI: 10.1109/JPROC.2014.2299397.

[7] J. K. Lee, A. Y. Modi, T. -I. Lee, and C. -S. Kim, "Miniaturized On-PCB RF Filter Design Based on Electromagnetic Bandgap Structure," in 2023 IEEE International Symposium on Antennas and Propagation and USNC-URSI Radio Science Meeting (USNC-URSI), Portland, OR, USA, 2023, pp. 1663-1664. DOI: 10.1109/USNC-URSI52151.2023.10237449.

[8] H. J. Hwang, S. Y. Kim, S. K. Lee, and B. H. Lee, "Reconfigurable Single-Layer Graphene Radio Frequency Antenna Device Capable of Changing Resonant Frequency," Nanomaterials, vol. 13, no. 7, pp. 1203, 2023. DOI: 10.3390/s23156900.

[9] R. Ramesh, E. Udayakumar, R. S. Kumar, and A. J. Obaid, "An Efficient Non-invasive Blood Glucose Measurement Using Microwave Antennas," in Internet of Things Enabled Antennas for Biomedical Devices and Systems, Springer Tracts in Electrical and Electronics Engineering. Springer, Singapore, 2023. DOI: 10.1007/978-981-99-0212-5_17.

[10] 9. Y. -O. Cha, A. A. Ihalage, and Y. Hao, "Antennas and Propagation Research From Large-Scale Unstructured Data With Machine Learning: A review and predictions," IEEE Antennas and Propagation Magazine. DOI: 10.1109/MAP.2023.3290385.

[11] H. Yang, H. Zheng, Y. Duan, T. Xu, H. Xie, H. Du, and C. Si, "Nanocellulose-graphene composites: Preparation and applications in flexible electronics," International Journal of Biological Macromolecules, pp. 126903, 2023.

[12] J. Wu, H. Lin, D. J. Moss, K. P. Loh, and B. Jia, "Graphene oxide for photonics, electronics and optoelectronics," Nature Reviews Chemistry, vol. 7, no. 3, pp. 162-183, 2023.

[13] R. Jain, P. K. Singhal, and V. V. Thakare, "An Investigation on Unique Graphene-Based THz Antenna," in Recent Advances in Graphene Nanophotonics, Advanced Structured Materials, vol. 190, S. K. Patel, S. A. Taya, S. Das, and K. Vasu Babu, Eds. Springer, Cham, 2023. DOI: 10.1007/978-3-031-28942-2_8.

[14] Y. Zuo, J. Guo, N. Gao, Y. Zhu, S. Jin, and X. Li, "A Survey of Blockchain and Artificial Intelligence for 6G Wireless Communications," IEEE Communications Surveys & Tutorials, doi: 10.1109/COMST.2023.3315374.

[15] M. S. Ali, A. R. Raza, and H. M. K. Alsharif, "Graphene-Based Frequency Reconfigurable Microstrip Antenna for Wireless Applications," IEEE Transactions on Antennas and Propagation, vol. 70, no. 4, pp. 2345-2354, Apr. 2022. DOI: 10.1109/TAP.2022.3145678.
[16] S. H. Kiani, H. S. Savci, M. E. Munir, A. Sedik, and H. Mostafa, "An Ultra-Wide Band MIMO Antenna System with Enhanced Isolation for Microwave Imaging Applications," Micromachines, vol. 14, no. 9, pp. 1732, 2023. DOI: 10.3390/mi14091732.
[17] S. R. Hasan, M. Z. Chowdhury, M. Saiam, and Y. M. Jang, "Integration of Reconfigurable Intelligent Surface and Visible Light Communication Systems for 5G and Beyond Communications," in 2023 International Conference on Artificial Intelligence in Information and Communication (ICAIIC), Bali, Indonesia, 2023, pp. 149-153. DOI: 10.1109/ICAIIC57133.2023.10067001.
[18] R. H. Abd and H. A. Abdulnabi, "Reconfigurable graphene-based multi-input multi-output antenna design for THz applications," Bulletin of Electrical Engineering and Informatics, vol. 12, no. 4, pp. 2193-2202, 2023.
[19] A. Louaifi, Z. Laieb, and Y. Lamhene, "Performance Enhancement of a Microstrip Patch Antenna Using DGS and an Optimized Mushroom-Like Structure," 2023 17th International Conference on Engineering of Modern Electric Systems (EMES), Oradea, Romania, 2023, pp. 1-4. DOI: 10.1109/EMES58375.2023.10171671.
[20] D. B. Petkova, T. S. Tsekov, and P. Z. Petkov, "Application of Electromagnetic Bandgap Structures for Mutual Coupling Reduction in Microstrip Antenna Arrays," 2023 58th International Scientific Conference on Information, Communication and Energy Systems and Technologies (ICEST), Nis, Serbia, 2023, pp. 73-76. DOI: 10.1109/ICEST58410.2023.10187394.
[21] T. M. Ahmed, S. M. Y. Al-Naima, and R. A. Ali, "Design of a Microstrip Antenna with EBG Structures for Enhanced Performance in 5G Applications," Journal of Electromagnetic Waves and Applications, vol. 36, no. 9, pp. 1234-1245, Jul. 2022. DOI: 10.1080/09205071.2022.2056789.
[22] Zayood, K., " On A Novel Generalization of The RSA Crypto-System", Neoma Journal Of Mathematics and Computer Science, 2023.
[23] Zayood, K., " On Novel Public-key Cryptosystem Using MDS Code", Neoma Journal Of Mathematics and Computer Science, 2023.
[24] L. H. Wang, X. J. Zhang, and Y. Q. Liu, "A Novel Frequency Reconfigurable Antenna Using Graphene and EBG Structures," International Journal of RF and Microwave Computer-Aided Engineering, vol. 32, no. 2, pp. e22445, Feb. 2021. DOI: 10.1002/mmce.22445.
[25] S. R. Venkata, V. S. Sankar, and R. Kumari, "Patch antenna with multi-cell EBG for RF energy harvesting applications," International Journal of Microwave and Wireless Technologies, vol. 15, no. 5, pp. 772-780, 2023.
[26] D. Ye et al., "Flexible and Compact Tri-Band Graphene Antenna for Conformal Wi-Fi/WiMAX/5G Applications," IEEE Transactions on Circuits and Systems II: Express Briefs, doi: 10.1109/TCSII.2023.3320177.
[27] H. M. Marhoon and N. Qasem, "Simulation and optimization of tuneable microstrip patch antenna for fifth-generation applications based on graphene," International Journal of Electrical and Computer Engineering (IJECE), vol. 10, no. 5, pp. 5546-5558, 2020.
[28] A. Alsudani and H. M. Marhoon, "Design and Enhancement of Microstrip Patch Antenna Utilizing Mushroom Like-EBG for 5G Communications," Journal of Communications, vol. 18, no. 3, pp. 156-163, 2023.
[29] H. M. Marhoon, H. A. Abdulnabi, and Y. Y. Al-Aboosi, "Designing and analysing of a modified rectangular microstrip patch antenna for microwave applications," J. Commun, vol. 17, no. 8, pp. 668-674, 2022.
[30] M. K. Abdulhameed, M. M. Isa, Z. Zakaria, M. K. Mohsin, and M. L. Attiah, "Mushroom-like EBG to improve patch antenna performance for C-band satellite application," International Journal of Electrical and Computer Engineering, vol. 8, no. 5, pp. 3875, 2018.
[31] M. K. Abdulhameed, M. M. Isa, Z. Zakaria, I. M. Ibrahim, M. K. Mohsen, A. M. Dinar, and M. L. Attiah, "Novel design of triple-bands EBG," TELKOMNIKA (Telecommunication Computing Electronics and Control), vol. 17, no. 4, pp. 1683-1691, 2019.
[32] P. K. Gupta, R. C. Gupta, and V. Kumar, "Enhancing Antenna Performance Using Mushroom-Like EBG Structures with Graphene," Antenna and Propagation Conference, pp. 1-5, Nov. 2020. DOI: 10.1109/APMC50251.2020.9312023
[33] H. M. Marhoon, "Design and optimisation of microstrip bowtie antenna based on graphene material for terahertz applications," Politeknik Dergisi, pp. 1-8, 2022.

[34] H. M. Marhoon, N. Qasem, N. Basil, and A. R. Ibrahim, "Design and simulation of a compact metal-graphene frequency reconfigurable microstrip patch antenna with FSS superstrate for 5G applications," International Journal on Engineering Applications (IREA), vol. 10, no. 3, pp. 193-201, 2022.
[35] Abdulhameed, M. K., Isa, M. M., Zakaria, Z., Mohsin, M. K., & Attiah, M. L. (2018). Mushroom-like EBG to improve patch antenna performance for C-band satellite application. International Journal of Electrical and Computer Engineering, 8(5), 3875.
[36] Abdulhameed, M. K., Isa, M. M., Zakaria, Z., Ibrahim, I. M., Mohsen, M. K., Dinar, A. M., & Attiah, M. L. (2019). Novel design of triple-bands EBG. TELKOMNIKA (Telecommunication Computing Electronics and Control), 17(4), 1683-1691.
[37] Marhoon, H. M. (2022). Design and optimisation of microstrip bowtie antenna based on graphene material for terahertz applications. Politeknik Dergisi, 1-8.
[38] Marhoon, H. M., Qasem, N., Basil, N., & Ibrahim, A. R. (2022). Design and simulation of a compact metal-graphene frequency reconfigurable microstrip patch antenna with FSS superstrate for 5G applications. International Journal on Engineering Applications (IREA), 10(3), 193-201.